Direct Tests of Muscle Cross-Bridge Theories: Predictions of a Brownian Dumbbell Model for Position-Dependent Cross-Bridge Lifetimes and Step Sizes with an Optically Trapped Actin Filament

D. A. Smith
The Randall Institute, King's College, London WC2B 5RL, United Kingdom

ABSTRACT Force and displacement events from a single myosin molecule interacting with an actin filament suspended between optically trapped beads (Finer, J. T., R. M. Simmons, and J. A. Spudich. 1994. *Nature.* 368:113–119) can be interpreted in terms of a generalized cross-bridge model that includes the effects of Brownian forces on the beads. Steady-state distributions of force and displacement can be obtained directly from a generalized Smoluchowski equation for Brownian motion of the actin-bead "dumbbell," and time series from Monte Carlo simulations of the corresponding Langevin equation. When the frequency spectrum of Brownian motion extends beyond cross-bridge transition rates, the inverse mean lifetimes of force/displacement pulses are given by cross-bridge rate constants averaged over a Boltzmann distribution of Brownian noise. These averaged rate constants reflect the strain-dependence of the rate constants for the stationary filament, most faithfully at high trap stiffness. Hence, measurements of the lifetimes and displacements of single events as a function of the resting position of the dumbbell can provide a direct test of different cross-bridge theories of muscle contraction. Quantitative demonstrations are given for Huxley models with 1) faster binding or 2) slower dissociation at positive cross-bridge strain. Predictions for other models can be inferred from the averaging procedure.

INTRODUCTION

Unitary force and displacement steps have been observed from interactions between single tethered molecules of the muscle proteins heavy meromyosin and a 3–10-μm actin filament, the latter held either by micron-sized latex beads in the double laser trap (Finer et al., 1994) or by a microneedle (Ishijima et al., 1991, 1996). Their existence confirms that muscle force arises from the summation of individual force-producing events between an actin filament and one myosin molecule, as suggested by A. F. Huxley (1957) and evidenced by Gordon et al. (1966). Hence, it is reasonable to assume that these events occur independently, so that the amplitudes and durations of these events characterize muscle action at the level of single-molecule interactions rather than the half-sarcomere. The half-sarcomere response sums contributions from cross-bridges with a wide distribution of kinetics arising from the vernier spacings of myosin heads (42.9 nm) and available actin sites (38.5 nm) (Huxley, 1957), and observations on fibers or myofibrils are usually reproduced in each half-sarcomere. There is a large body of evidence for the hypothesis that muscle contraction arises from strain-dependent cross-bridge transitions (Hibberd and Trentham, 1986; Cooke, 1987, 1997).

Experimental displacement-time series show random fluctuations consistent with the Brownian motion of the actin-bead system, or "dumbbell," as well as discrete events at random intervals from interaction with one or more myosin molecules bound to a coverslip. In the limit of low myosin density, these events appear as steps and arise from the binding or dissociation of probably just one myosin-S1 head (Molloy et al., 1995b). To interpret these experiments it is necessary to have a model in which cross-bridge transitions and Brownian forces on the beads are treated on an equal footing. Myosin binding/dissociation changes the subsequent Brownian motion of the dumbbell; the nature of this motion can affect the incidence of cross-bridge transitions (Block and Svoboda, 1995; Molloy and White, 1997), and can therefore be used as a tool for modifying the behavior of the cross-bridge, for example by changing the stiffness of the traps. Modulation of cross-bridge kinetics by translational motion of filaments also explains why the cross-bridge duty cycle in muscle is a strong function of the load (Huxley, 1957).

Such a model is presented in the next section. The simplest cross-bridge cycle (Huxley, 1957) is used for ease of presentation, since the generalization to a comprehensive actin-myosin cycle is straightforward. The model can be written in terms of a Langevin equation of motion and, more powerfully, as a generalization of Smoluchowski's equation for the displacement distribution to include cross-bridge states (section 3). Steady-state solutions of the latter can be generated numerically. Very simple analytic solutions (section 4) exist when, as is usually the case, the correlation times of Brownian motions of the dumbbell are much less than the lifetimes of cross-bridge states. Then these motions achieve their equilibrium (or Boltzmann) distribution within the lifetime of each cross-bridge "level," and the effective transition rates between levels are averages of the strain-dependent rate constants used for models of the muscle sarcomere (Smith and Geeves, 1995).

Received for publication 7 January 1998 and in final form 27 August 1998.
Address reprint requests to Dr. David Smith, The Randall Institute, King's College, 26–29 Drury Lane, London WC2B 5RL, United Kingdom. Tel.: 44-1-71-465-5404; Fax: 44-1-71-497-9078; E-mail: dave@muscle.rai.kcl.ac.uk.

0006-3495/98/12/2996/12 $2.00

This result provides a deeper connection between single-molecule experiments and the strain-dependent kinetics of muscle contraction, and suggests new ways of testing models of contraction. The net rate of escape from a level is the inverse of the mean lifetime of the level (Colquhoun and Hawkes, 1977), which is experimentally available (Guilford et al., 1997). At high trap stiffness, the strain-dependences of the rate constants are little affected by Brownian averaging, and can be explored by measuring mean lifetimes as a function of the resting position of the dumbbell with respect to the myosin molecule. If observed levels in force/displacement records are associated with distinct states of a cross-bridge cycle, strain-dependent rate constants as required for muscle cross-bridge theories can be reconstructed directly from single-molecule force data at different trap positions. Examples using Huxley models are presented in section 4. These effects can be glimpsed in preliminary results of Molloy et al. (1995a) with a driven sinusoidal displacement of the traps.

Related experiments on the kinesin-microtubule motor also reveal step events (Svoboda et al., 1993), but of a different kind (Svoboda et al., 1994). The processive motion of kinesin and related motors apparently requires two-headed motor molecules with some cooperation between the two heads, and semi-phenomenological models have been proposed, for example by Peskin and Oster (1995) and Derenyi and Vicsek (1996). The relation of these models to the biochemical kinesin-microtubule-ATP cycle (Gilbert et al., 1995; Ma and Taylor, 1997) is not yet clear, but the methods of this paper might also be applied to kinesin-microtubule motors.

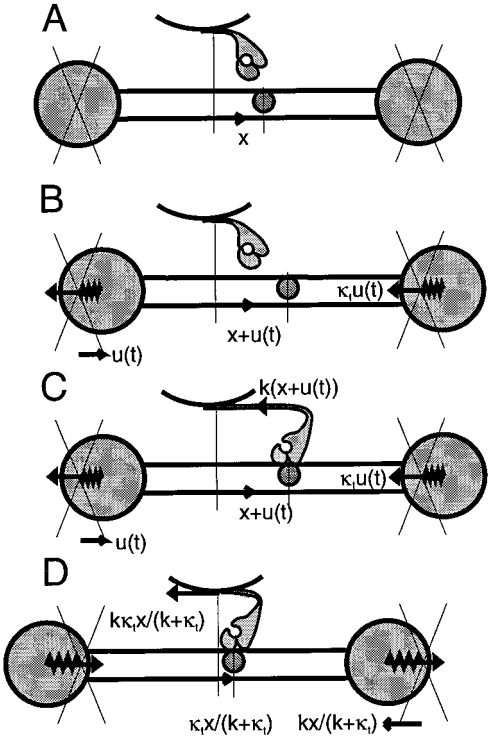

FIGURE 1 Schematic configurations in the double laser-trap experiment, showing two optically trapped latex beads connected by an actin filament and one S1-myosin molecule tethered to a fixed coverslip. For simplicity, only one binding site on actin is shown, also just one free and one bound myosin state (Huxley, 1957). (*A*) The resting position of the "dumbbell" with actin site at distance x to the right of a reference position in the myosin head. (*B*) A thermally generated displacement $u(t)$ of the dumbbell, resisted by the restoring force $\kappa_t\, u(t)$ from the traps, moves the site to $x + u(t)$ while the head stays free. (*C*) Myosin binding to at this displacement gives an extra left-directed force $k(x + u(t))$ on the dumbbell (the diagram does not illustrate that binding is likely only when $x + u(t)$ is within some binding range). (*D*) The dumbbell moves to its equilibrium resting position $u = -kx/(k + \kappa_t)$ in which the forces $k(x + u)$ and $\kappa_t u$ are equal and opposite. Brownian forces also cause displacement fluctuations (not shown) about this position. Displacements are marked by open arrows and forces by filled arrows.

THE BROWNIAN DUMBBELL MODEL

A simple but realistic model for the double-bead experiment can be constructed by treating the actin-bead system as a rigid dumbbell moving under elastic restoring forces from the traps and cross-bridge, plus viscous drag and Brownian forces acting on the beads. The tethered head is assumed to be a single myosin-S1 molecule. Only longitudinal forces and motions are treated explicitly. Brownian motions of the detached myosin head and internal motions of the actin filament can be incorporated within effective cross-bridge binding and dissociation rates as their time scales are below the correlation time of longitudinal displacement noise (typically 0.1–1 ms). The actin filament itself is almost inextensible compared with the cross-bridge, and lateral displacements of a filament with fixed ends can be ignored, so the compliance of the actin-bead links is of more concern. However, torsional motions in the actin filament are expected. A full discussion is given in the last section of this paper.

The model can be understood in mechanical terms using Fig. 1, which summarizes the geometry and the restoring forces, assuming that the head contains a linear elastic element (Ford et al., 1977). Fig. 1 *A* defines the geometry of the dumbbell at rest, with a binding site at distance x from the tethered myosin. The traps exert a restoring force when the dumbbell is displaced by Brownian forces on the beads (Fig. 1 *B*), with an extra restoring force when myosin binds (Fig. 1 *C*). If the head remains bound, the dumbbell moves to balance the forces from the traps and cross-bridge, giving a different resting position of the dumbbell (Fig. 1 *D*). Additional random displacements from Brownian forces can be expected at any instant, so that in experimental records each resting position is obscured by displacement noise and must be defined as a local mean displacement, or "level." The size of the step produced when myosin binds to a force-producing state is the difference between the two levels, with an equal and opposite step if the head dissociates from the same state. The noise variance should be smaller after binding because the net stiffness of the dumbbell has increased, and the observation of this effect by

Molloy et al. (1995a, b) supports this interpretation of displacement steps.

When the traps are much more compliant than the cross-bridge, the step produced on binding is equal to the working stroke of the cross-bridge, defined as the filament displacement (initial tension/stiffness) required to reduce its tension to zero in the absence of any kinetic change. For simplicity, head-filament interactions use one detached state and one bound state per site. If force is generated by a two-stage process (Huxley and Simmons, 1971) the total working stroke is the sum of a binding stroke to relieve the initial tension and a force-generating stroke to relieve extra tension created by a conformational change of the myosin neck (Holmes, 1997).

The number of actin sites available for binding may be limited by their orientation on the double-helix, which provides some degree of azimuthal selection (Molloy et al., 1995a) within each half-pitch (38.5 nm), but it is not clear whether the filament rotates to present additional sites, so the model is formulated by treating the number $2L + 1$ of adjacent sites ($L = 0, 1, 2, \ldots$) as a free parameter.

Let $u(t)$ be the longitudinal displacement at time t of the dumbbell. It is moved by the restoring force of the optical traps with equivalent elastic stiffness κ_t, viscous drag with coefficient β from dumbbell motion in the surrounding fluid of viscosity η, a net random Brownian force $F_B(t)$ on both beads, and cross-bridge tension T in the direction of negative-x when the head is bound to the filament. The drag force arises mostly from the beads, so $\beta \approx 2(6\pi\eta a)$ for beads of radius a. The combined mass is small enough that inertial forces can be neglected. Hence the Langevin equation of motion is

$$\beta \frac{\mathrm{d}u}{\mathrm{d}t} + \kappa_t u(t) = F_B(t) - T(x + u(t), t) \qquad (1)$$

where T is shown as a function of the displacement x of the central actin site from the resting position of the head. The value of x is set by the position of the traps with respect to myosin, and this displacement becomes $x + u$ when the dumbbell is displaced. Cross-bridge tension arises when S1-myosin binds to one site only, and is given by

$$T(x, t) = \sum_{l=-L}^{L} k(x + lc) n_l(t),$$

$$n_l(t) = \begin{cases} 1, & \text{head bound to site } l \\ 0, & \text{otherwise} \end{cases} \qquad (2)$$

for cross-bridge stiffness k and $2L + 1$ possible binding sites spaced by $c = 5.5$ nm. There are $2L + 2$ cross-bridge states. The origin of x is defined so that tension from the central site is kx. The transition probabilities for binding and dissociation are $f(x + lc + u(t))$ and $g(x + lc + u(t))$ where the functions $f(x)$ and $g(x)$ define a two-state cross-bridge model (Huxley, 1957). When trap stiffness is low, the dumbbell may move over more than one half-pitch of the actin double helix. This can be incorporated by shifting $x + u(t)$ up or down by 38.5 nm, since clusters of sites separated by 38.5 nm are too widely separated to compete for the same head.

This model contains two stochastic processes, bindings and detachments of the head to and from actin as a Markov process controlled by the above transition probabilities, and the random force on the beads produced by collisions with solvent molecules. Brownian force noise is uncorrelated on virtually any time scale and therefore has a flat "white noise" power spectrum. Classical arguments imply that the variance of the Brownian force is infinite, so the correlation function can be written using a Dirac delta function as

$$\overline{F_B(t)F_B(t')} = C\delta(t - t'), \qquad (C = 2\beta\mathrm{RT}). \qquad (3)$$

The relation between C and the drag coefficient β arises from the law of equipartition of energy. It is easily verified from a formal solution of the Langevin equation by equating the mean potential energy of the noisy dumbbell in the traps to RT/2, where R is Boltzmann's constant and T the absolute temperature (Reif, 1965). The dumbbell model is now fully specified.

The model can be extended to include compliant linkages between filament and beads, which can be of the same order as cross-bridge compliance or less. Separate equations of motion can then be set up for longitudinal motions of the filament and each bead (Appendix A). As viscous drag on the filament can be neglected, the Appendix shows that the symmetric mode of motion of the beads is controlled by a Langevin equation equivalent to Eq. 1, but with an apparent cross-bridge stiffness including actin-bead linkages in series with the cross-bridge. For reference, mathematical symbols are collated in Table 1.

Monte Carlo simulations

The simplest method of exploring the dumbbell model is through Monte Carlo simulations, which generate Brownian force and cross-bridge transitions in time. The price of simplicity is that the time interval Δ between successive moves must be much less than the damping time and the lifetimes of cross-bridge states, and many Monte Carlo runs are needed to build up displacement distributions. On integrating the Langevin equation (Eq. 1) from time $t_n = n\Delta$ (n integral) to t_{n+1} where $\lambda(t_n)\Delta \ll 1$, the next displacement is

$$u(t_{n+1}) = (1 - \lambda(t_n)\Delta)u(t_n) + (1/\beta)\{\mathbf{B}(t_n) - T(x, t_n)\Delta\} \qquad (4)$$

where

$$B(t_n) = \int_{t_n}^{t_{n+1}} F_B(t)\,\mathrm{d}t, \qquad \lambda(t) = \frac{\kappa_t + \mathrm{k}(t)}{\beta}. \qquad (5)$$

B is an "impulse" integral of Brownian force over time Δ, and is a random variable with a finite variance

$$\overline{B(t_n)^2} = C\Delta = 2\beta^2 D\Delta \qquad (D = RT/\beta). \qquad (6)$$

TABLE 1 Digest of mathematical symbols

Symbol	Definition
A	Attempt frequency
a	Bead radius
$B(t)$	Impulse integral of Brownian force
c	Actin monomer spacing
C	Correlation coefficient of Brownian force ($C = 2\beta$RT)
D	Diffusion constant of dumbbell ($D = \mathrm{RT}/\beta$)
$F_B(t)$	Brownian force on both beads
$\underline{f(x)}$, $\underline{g(x)}$	Binding and dissociation rates of actin-myosin
$\overline{f(x)}$, $\overline{g(x)}$	Brownian-averaged rates
$J_i(u, t)$	Dumbbell flux (net velocity X $P_i(u, t)$)
k	Crossbridge stiffness
k(t)	k$n(t)$
$K(x)$	$f(x)/g(x)$
l	Actin site label ($l = -L, L$) in cluster
$2L + 1$	Number of actin sites available in cluster
$\mathbf{M}(x)$	Reaction matrix ($M_{11} = -M_{21} = f(x)$, $M_{22} = -M_{12} = g(x)$)
$n(t)$	Actin-myosin binding index (0 or 1)
$p_i(x)$	Probability of crossbridge state i
$P_i(u, t)du$	Probability of crossbridge state i and displacements (u, $u + du$)
R	Boltzmann's constant
t	Time
$t_i(x)$	Crossbridge tension in state i
T	Absolute temperature
$T(x, t)$	Crossbridge tension at time t
u	Dumbbell displacement
$U_l(x)$	Mean displacement of bound level to actin site l
$V_1(u)$	Potential energy of traps at displacement u
$V_2(u, x)$	Potential energy of traps and bound myosin, displacement u
x	Resting position of actin site from myosin
β	Viscous damping coefficient of both beads ($\beta = 12\pi\eta a$)
κ_t	Combined stiffness of both traps
λ_t	Damping frequency (rads/s) of free dumbbell
λ	Damping frequency of dumbbell with bound myosin
η	Solution viscosity
$\varphi_1(u)$	Boltzmann displacement distribution of free dumbbell
$\varphi_2(u, x)$	Boltzmann distribution of dumbbell with bound myosin
$\tau_i(x)$	Lifetime of crossbridge state i

using Eq. 3. An application of the central limit theorem shows that the distribution of B is Gaussian (Chandrasekhar, 1943). Working with this "impulse" function avoids mathematical difficulties associated with the unaveraged Brownian force (Gardner, 1985). Here D is the diffusion constant connected by Einstein's relation to the damping coefficient, and the random term B/β is a diffusive displacement with a Gaussian distribution of zero mean and variance $2D\Delta$ (the classical diffusion law). This algorithm has been used for motility assays (Brokaw, 1976; Pate and Cooke, 1991) where the diffusion is unconstrained by trap forces.

Monte Carlo simulation can proceed using a Gaussian random number generator for values of B, and a separate generator of a uniformly distributed random number r between 0 and 1 (Press et al., 1992) for each cross-bridge transition. For a detached head, binding to site l is allowed if and only if r is less than the binding probability over time Δ, with a corresponding rule if the head is initially bound. $f(x + lc + u(t_n))\Delta$ and $g(x + lc + u(t_n))\Delta$ are the probabilities of binding and dissociation, neglecting the change in displacement over that time. This algorithm is valid if

$$\lambda(t)\Delta \ll 1, \qquad f\Delta, g\Delta \ll 1. \tag{7}$$

The first inequality requires many Monte Carlo steps before the dumbbell comes to equilibrium in its potential well. This condition is very restrictive, giving large amounts of output correlated over time of order $1/\lambda$. Hence, redundant output should be thinned before writing to a file. However, the algorithm itself is fast and therefore runs of 10^7 steps are quite feasible. Results obtained with Eqs. 4–7 are shown in Fig. 2 for a modified Huxley model described in the caption, using $\Delta \leq 10^{-6}$ s and $\mathrm{k}/\beta = 2 \times 10^4\ \mathrm{s}^{-1}$ from Table 2. The basic features of these simulations are

- After a single head binds to the filament, the mean level of the displacements jumps from zero to $u = U_f(x) \equiv -\mathrm{k}(x + lc)/(\mathrm{k} + \kappa_t)$, for which tensions $\mathrm{k}(x + lc + u)$ and $\kappa_t u$ from the head and trap are equal and opposite;
- The variance of displacements centered about zero is RT/κ_t when the head is detached, and the variance about the level $U_f(x)$ is $\mathrm{RT}/(\mathrm{k} + \kappa_t)$;
- With low trap stiffness ($\kappa_t \ll \mathrm{k}$) the duty cycle or ratio of "on" times to "off" times will be much lower than f/g if the amplitude of Brownian motion in the detached state exceeds the binding range defined by $f(x)$.

It is desirable to have Monte Carlo algorithms for use with larger sampling times, say $\Delta \geq 1/\lambda$. In this case, Brownian motion of the dumbbell between Monte Carlo steps will be significant, so that each cross-bridge transition may occur with different rates at different times in the interval Δ. Hence, the prediction problem must be solved within each time interval as well as from one Monte-Carlo step time to the next. Fortunately, stochastic predictions can be made analytically when Brownian motion is fast relative to cross-bridge transition rates. This requires a complete statistical description of the dumbbell motion, which will be presented elsewhere.

THE GENERALIZED SMOLUCHOWSKI EQUATIONS

The dynamics of the dumbbell–cross-bridge system is controlled by two interacting Markov processes for Brownian motion and cross-bridge transitions, respectively. The Brownian motion of a single spherical particle can be predicted in the statistical sense from the conditional probability distribution of its x-displacement u at time t, given a displacement u_o at an earlier time t_o. This motion has the Markov property that no history of previous displacements is relevant, since the change in displacement is determined by random force noise acting over the intervening period and any change in cross-bridge tension. Each cross-bridge transition is assumed to be instantaneous on the time scales considered here. The conditional distribution obeys Smoluchowski's equation (Chandrasekhar, 1943), which is a spe-

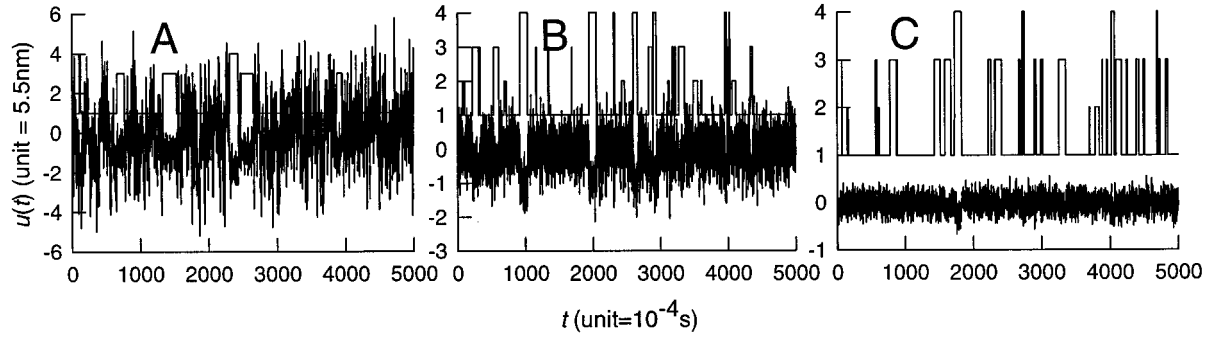

FIGURE 2 Sample Monte Carlo simulations made from Eqs. 5–7 using a modified Huxley model (Model I), three adjacent actin sites spaced by 5.5 nm, and three values $\kappa_t/k = 0.1$ (*A*), 1.0 (*B*), and 10 (*C*) of the ratio of trap to cross-bridge stiffness. The model is defined by a strain-dependent binding rate $f(x) = f\exp(-a_1x - a_2x^2 - a_4x^4)$ with $f = 10\ s^{-1}$, $a_1 = -3.0$, $a_2 = 2.0$ and $a_4 = 0.2$, which favors positive strains, while $g(x) = 200\ s^{-1}$ is constant. Tension satisfies Eq. 2 with k = 0.53 pN/nm. The unit of length is $c = 5.5$ nm and kc = 2.91 pN is the unit of force, giving $\beta = 5 \times 10^{-5}$ units and $\lambda_t = 2000\ s^{-1}$, $\lambda = 22000\ s^{-1}$ (Table 2). Calculations were made for $x = 5.5$ nm (1 length unit). The step time satisfied condition (8) by a factor of at least five. Displacements were recorded every 0.1 ms, also the sequence of cross-bridge states (1–4). The bound states (2–4) have $l = -1,0,1$, respectively, and their levels are as stated in the main text. Values of f and g were chosen to give duty ratios and lifetimes similar to published data at high ATP levels. Note that the difference between the mean levels of the two states and the noise variance in the off state are decreasing functions of trap stiffness, but the duty ratio increases.

cial case for overdamped particles of a Fokker-Planck equation for the distribution of position and velocity.

Smoluchowski's equation can be generalized in an obvious way to include the cycles of one or more interacting myosin heads, by specifying the cross-bridge state simultaneously with the displacement. Let $P_j(u, t)du$ be the probability of displacements in the range $(u, u + du)$ at time t and cross-bridge state j, not listing the initial conditions. For multiple actin sites, the cross-bridge state should includes a site index l as before. In this case we have "Smoluchowski-Huxley" equations

$$\frac{\partial P_1(u,t)}{\partial t} = \frac{1}{\beta}\frac{\partial}{\partial u}\left(\frac{\partial V_1(u)}{\partial u}P_1\right) + D\frac{\partial^2 P_1}{\partial u^2} + \sum_{l=-L}^{L}\left(g(x+lc+u)P_{2l} - f(x+lc+u)P_1\right)$$

$$\frac{\partial P_{2l}(u,t)}{\partial t} = \frac{1}{\beta}\frac{\partial}{\partial u}\left(\frac{\partial V_{2l}(u)}{\partial u}P_{2l}\right) + D\frac{\partial^2 P_{2l}}{\partial u^2} + f(x+lc+u)P_1 - g(x+lc+u)P_{2l} \tag{8}$$

for the dumbbell moving in different elastic potentials

$$V_1(u) = \frac{1}{2}\kappa_t u^2, \qquad V_{2l}(u) = \frac{1}{2}[\kappa_t u^2 + k(x+lc+u)^2] \tag{9}$$

for each state. Note that the stiffness of the dumbbell with bound cross-bridge is $k + \kappa_t$ (elastic elements in parallel) if forcibly displaced at fixed x. However, the stiffness with respect to a forcible change in x (by moving the traps or the coverslide) is $k\kappa_t/(k + \kappa_t)$ (elements in series), which changes the stable position $u = -kx(k + \kappa_t)$ of the dumbbell. Completeness is expressed by a sum rule over final states

$$\sum_j \int du\, P_j(u,t)\, du = 1. \tag{10}$$

Equations 8 can be formally derived from the Langevin equation and the usual stochastic interpretation of the cross-bridge rate constants (Chandrasekhar, 1943; Doi and Edwards, 1988). They reduce to Smoluchowski's equation in the absence of cross-bridge transitions, and to the usual chemical-kinetic equations in the absence of Brownian motion ($D = 0$). The following statement may assist readers not familiar with Smoluchowski's equation: the first two terms on each right-hand side can be written as minus the u-derivative of a flux, arising from damping-limited drift in the force of the elastic potential and from diffusion (Appendix B). The Einstein relation in Eq. 6 ensures that the solution of Smoluchowski's equation tends to the correct

TABLE 2 Parameter values for the Brownian dumbbell model

Primary	Derived
$a = 0.55\ \mu$m, $\eta = 1.0 \times 10^{-3}$ N · s · m^{-2}	$\beta = 12\pi\eta a = 2.07 \times 10^{-8}$ N · s · m^{-1}
$c = 5.5$ nm	$\lambda_t = \kappa_t/\beta = 2420\ s^{-1}$ (damping frequency)
$f = 10\ s^{-1}$ (models I and II)	$\lambda = (k + \kappa_t)/\beta = 26600\ s^{-1}$
$g = 200\ s^{-1}$	$(RT/\kappa_t)^{1/2} = 8.94$ nm (standard devn.)
k = 0.5 pN/nm (Smith and Geeves, 1995)	$(RT/(k + \kappa_t))^{1/2} = 2.70$ nm
RT = 4×10^{-21} J at 17°C	$\kappa_t(RT/(k + \kappa_t))^{1/2} = 4.26$ pN ($\kappa_t = 10$ k)
$\kappa_t = 0.1$ k (no feedback)	$D = RT/\beta = 1.93 \times 10^{-13}$ m^2/s

equilibrium form (a Boltzmann distribution) at large times. Although the drift and diffusion terms disappear on integrating over u, closed equations for the probabilities of cross-bridge states cannot be obtained in this way except for the unphysical case where $f(x)$ and $g(x)$ are independent of x, when Huxley's equations with no additional noise terms are recovered. To add phenomenological noise terms to the Huxley equations, as was done by Thomas and Thornhill (1995), is incompatible with this generalized Smoluchowski theory. Extra terms should not be expected since kinetic equations for the state probabilities already have a stochastic interpretation (Nicolis and Prigogine, 1977; Saldana and Smith, 1991).

These equations provide complete statistical predictions for the behavior of the Brownian dumbbell. In general, they must be solved numerically. A general analytic solution can be constructed if the time scales of Brownian motion and cross-bridge events are very different, but only steady-state solutions will be considered here.

The steady-state distribution of levels

Much effort has been devoted to obtaining the distribution of "levels" for records of single actin-myosin interactions (Molloy et al., 1995b, Guilford et al., 1997), a level being a region of constant local mean displacement. Binding events then appear as the transition from a high-variance level to a low-variance level, and the step size is defined as the difference in the mean displacements of each level. The advantages of using this definition are that any drag or push from Brownian forces is canceled in taking the mean displacements, and that at low trap stiffness ($\kappa_t \ll k$) the step size is equal to the myosin working stroke as defined earlier. Under conditions where only one head cycles at a time, this working stroke is equal to the "ATP step length" if one molecule of ATP is hydrolyzed by each cycle.

For constant bath conditions and no externally forced motion, a unique steady-state distribution of displacements is expected which is characteristic of the proteins, the trap stiffness and the resting position of the dumbbell. This distribution can be built numerically from Monte Carlo simulations, but can also be obtained directly from the generalized Smoluchowski equations (Fig. 3). For the latter, numerical methods are essential even when $f(x)$ and $g(x)$ are independent of x. The motion of the dumbbell is bounded with no net flux at large displacements, so $P_j(u)$ and its u-derivative must tend to zero as $u \to \infty$. A robust numerical method (Appendix B) confirms that the distributions remain close to Gaussian as f and g are increased up to viscoelastic damping frequencies, when cross-bridge transitions disturb the Boltzmann distribution of displacements.

The significance of the shift in level on binding can be tested by standard methods, which compare it with pre- and post-step variances. For example, for the same populations in each level, an F-test involves the square of the level shift divided by the sum of these variances (Weatherburn, 1968),

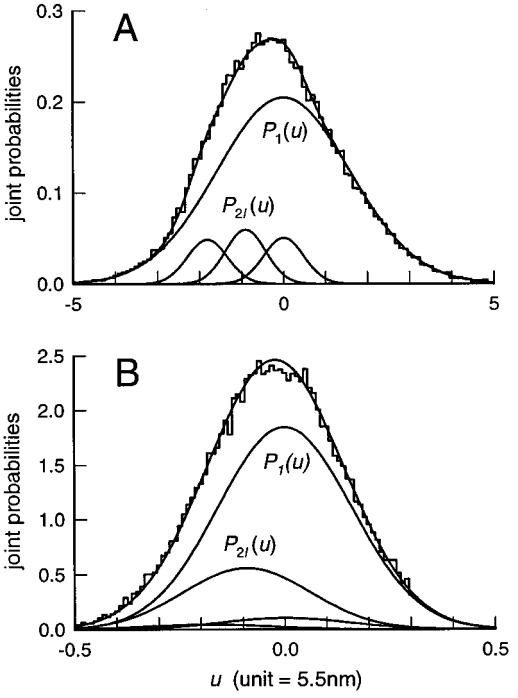

FIGURE 3 Joint probabilities for displacement and cross-bridge state for Huxley model I with three available actin sites and $x = 1$. The distribution $P_1(u)$ is for free myosin and $P_{2l}(u)$ for myosin bound to actin site $l = (-1,0,1)$, which appear from right to left in the figure with mean values given by Eq. 19. The displacement distribution obtained by summing over states is also shown unlabeled. The continuous curves are the numerical steady-state solution of the Smoluchowski-Huxley equations (8). Normalized histograms for the displacement distribution are built from corresponding Monte Carlo simulations with a total of 50,000 points (5 s duration), using displacement bins of width 0.1 units (A) and 0.01 (B): differences between each histogram and the theoretical distribution are as expected for sample counts of order 500 at $u = 0$. All results use model I and parameters of Fig. 2 with $\kappa_t/k = 0.1$ (A) and 10 (B). The step size on binding to site l (working strokes) is the shift in mean displacement between the two distributions. At high trap stiffness $\kappa_t/k \gg 1$ (B), the standard deviation of each distribution is reduced (as $k^{-1/2}$) but the working stroke is reduced even more (as k^{-1}), so the separation of these distributions is reduced. Note also that the actin site $l = 0$ is kinetically favored at high trap stiffness.

which for the central site is

$$\left(\frac{kx}{k+\kappa_t}\right)^2 \Big/ \left(\frac{RT}{\kappa_t}+\frac{RT}{k+\kappa_t}\right) \equiv \frac{k\kappa_t}{(k+\kappa_t)(k+2\kappa_t)}\frac{kx^2}{RT}. \quad (11)$$

As a function of trap stiffness for a given site location x, the two distributions are best separated when $\kappa_t = k/\sqrt{2}$, not with very high trap stiffness, as might have been expected. When $\kappa_t \gg k$ (achievable with negative-feedback modulation of the trap positions) all displacements are small so the traps act as force transducers and can be calibrated as such (Simmons et al., 1996). Nevertheless, cross-bridge force kx does not appear as a sharp peak in the measured force distribution, but as a small shift in the mean value of a broad distribution of cross-bridge force when the head is bound. The shift is small because the size $kx/(k + \kappa_t)$ of the displacement which mechanically equilibrates the dumbbell

is much smaller than the working stroke x, and is proportional to κ_t^{-1}. This reduction is built into the force calibration of the transducer, but the r.m.s. displacement noise from Brownian motion is proportional to $\kappa_t^{-1/2}$. Thus the unfiltered signal-to-noise ratio for $\kappa_t \gg k$ is also proportional to $\kappa_t^{-1/2}$, which is a decreasing function of trap stiffness (Simmons et al., 1993). For example, with $x = 5.5$ nm and parameters of Table 2, the F-quantity at $\kappa_t/k = 10$ is 0.173 and the standard deviation of force noise is 4.3 pN (second-to-last entry in Table 2), whereas its maximum value is 0.686 with a force noise of 0.77 pN. Since the corner frequency of force noise is proportional to κ_t, some improvement can be made by low-pass filtering, which increases F in proportion to the reduction in bandwidth (Svoboda and Block, 1994). However, specialized filters are required to transmit sharp edges without broadening (Block and Svoboda, 1995).

THE CASE OF FAST BROWNIAN MOTION

Gaussian distributions of displacements in each level are expected when the roll-off or "corner" frequencies of the power spectra of Brownian displacements in the free and bound states are faster than the rates of escape by cross-bridge transitions, that is

$$\lambda_t \gg f, \quad \lambda \gg g \quad \left(\lambda_t = \frac{\kappa_t}{\beta}, \lambda = \frac{k + \kappa_t}{\beta}\right). \tag{12}$$

For simplicity, head-filament interactions use one detached state and one bound state per site. For cross-bridge rates below 1000 s^{-1}, these conditions are reasonably well met in experiments using laser traps (typically $\lambda_t \sim 2000\ s^{-1}$, $\lambda \sim 10\lambda_t$ at low trap stiffness) and in Table 2. They allow the construction of approximate analytic solutions of the generalized Smoluchowski equations under steady-state and transient conditions. These results are essential for developing Monte Carlo algorithms valid for larger time steps, for relating the amplitudes of the steady-state Gaussian distributions of each level to cross-bridge kinetics, for predicting the lifetime of each level and for developing maximum-likelihood methods.

Equation 12 implies that the distribution of Brownian displacements of the dumbbell will usually come to equilibrium between successive bindings and detachments. Equilibrium (Boltzmann) distributions in each state are Gaussian distributions $\varphi_1(u)$ and $\varphi_{2l}(u) \equiv \varphi_2(u/x + lc)$ whose means and variances were given in section 2:

$$\varphi_1(u) = \left(\frac{\kappa_t}{2\pi RT}\right)^{1/2} \exp\left(-\frac{\kappa_t u^2}{2RT}\right) \tag{13a}$$

$$\varphi_2(u|x) = \left(\frac{k + \kappa_t}{2\pi RT}\right)^{1/2} \exp\left(-\frac{(k+\kappa_t)}{2RT}\left(u + \frac{kx}{k+\kappa_t}\right)^2\right) \tag{13b}$$

Hence, the steady-state probabilities $P_i(u\,x)$ for state i and displacement u are

$$P_1(u|x) = p_1(x)\varphi_1(u), \quad P_{2l}(u|x) = p_{2l}(x)\varphi_2(u|x + lc) \quad (l = -L, L), \tag{14}$$

(Fig. 3), and x is fixed by the geometry of the system (Fig. 1). The probability $p_i(x)$ of cross-bridge state i is determined by balancing the net rates of binding to and dissociation from each actin site when averaged over the Brownian motion, namely

$$\int_{-\infty}^{\infty} \{f(x + lc + u)P_1(u|x) - g(x + lc + u)P_{2l}(u|x)\}\, du = 0. \tag{15}$$

By integrating the steady-state Smoluchowski-Huxley Eqs. 8 over u, this condition follows from the requirement that the distributions and their first derivatives with respect to u vanish at large u. Hence, the state populations satisfy

$$\frac{p_{2l}(x)}{p_1(x)} = \tilde{K}(x + lc) \equiv \frac{\tilde{f}(x + lc)}{\tilde{g}(x + lc)}, \quad (p_1(x) + \sum_{l=-L}^{L} p_{2l}(x) = 1) \tag{16}$$

where

$$\tilde{f}(x) = \int_{-\infty}^{\infty} f(x+u)\varphi_1(u)\, du, \qquad \tilde{g}(x) = \int_{-\infty}^{\infty} g(x)\varphi_2(u|x)\, du. \tag{17}$$

Here $\tilde{f}(x + lc)$ and $\tilde{g}(x + lc)$ are the effective rates of binding to and dissociation from actin site l, averaged over a Boltzmann distribution of Brownian motions before the transition. When Eq. 12 applies, these averaged rates predict the lifetime of each level, and standard results from the theory of discrete Markov processes (Colquhoun and Hawkes, 1977) can be taken over without modification. For the multi-site Huxley model, each tension level is associated with only one state. Then the lifetime of each level is exponentially distributed (a Poisson distribution of order zero), and the mean lifetimes τ_1 and τ_{2l} are again functions of x and given by

$$\frac{1}{\tau_1(x)} = \sum_{l=-L}^{L} \tilde{f}(x + lc), \quad \frac{1}{\tau_{2l}(x)} = \tilde{g}(x + lc) \tag{18}$$

which amounts to an ergodic interpretation of Eq. 16 for the occupation probabilities. These relationships were checked by computing the displacement distributions (Eq. 14) using Eqs. 13, 16, and 17. For the parameters used in Fig. 3 the results are graphically indistinguishable from the direct solution of the Smoluchowski-Huxley equations shown in the

figure. However, differences appear if f and/or g are increased by a factor of 1000, which violates conditions (Eq. 12) for fast Brownian motion. To summarize, cross-bridge kinetics determine the occurrence of different levels, whereas the step size

$$U_l(x) = -\mathrm{k}(x + lc)/(k + \kappa_t) \qquad (19)$$

from the detached-state level to a bound-state level is determined by geometry and the elastic constants k, κ_t (section 2).

Brownian-averaged rate constants enable the x-dependence of the corresponding steady-state populations to be compared for different cross-bridge models, which cannot be readily distinguished from results at just one resting position of the dumbbell. For a two-state model, the comparisons that can be made are illustrated in Fig. 4 for two variations of the Huxley model in which the required kinetic asymmetry with respect to x is put either in the binding rate

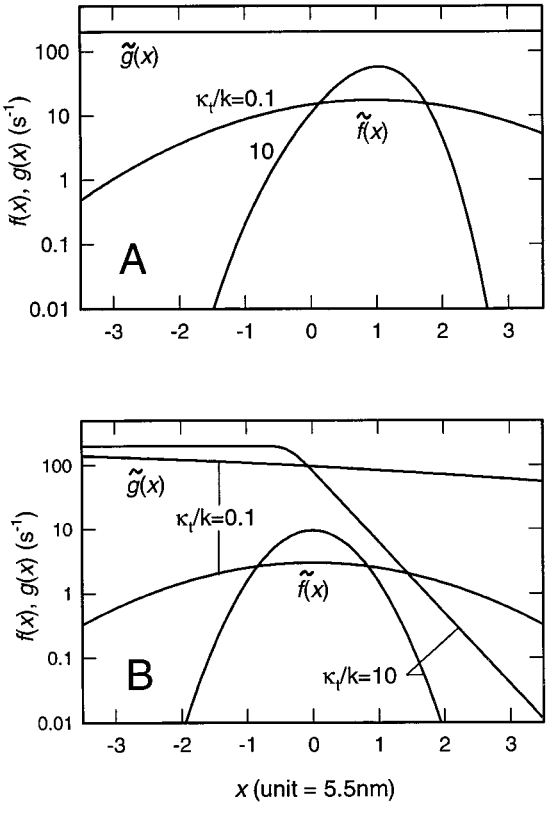

FIGURE 4 Brownian-averaged rate constants $\tilde{f}(x)$, $\tilde{g}(x)$ as a function of actin site position x and trap stiffness/cross-bridge stiffness κ_t/k for two contrasting versions of the Huxley model. (*A*) Model I with an asymmetric binding rate $f(x)$ biased toward positive x but a strain-independent dissociation rate g (see Fig. 2). (*B*) Model II, with a symmetric binding rate $f(x) = f \exp(-\mathrm{k}x^2/2\mathrm{RT})$ but a strain-dependent dissociation rate favoring negative strains, namely $g(x) = g$ for $x < x_\mathrm{I}$ or $g \exp(-b(x - x_\mathrm{I}))$ for $x < x_\mathrm{I}$ where $x_\mathrm{I} = -0.35$ (in units of 5.5 nm) and $b = 2.8$. These forms can be interpreted in terms of strain-blocked ADP release or ATP binding (Smith and Geeves, 1995). For high trap stiffness (κ_t/k = 10), the Brownian averaged rates are close to the unaveraged rate constants $f(x)$, $g(x)$ since the amplitude of the Brownian noise is small. At low trap stiffness the strain-dependence is small and the models are not so well differentiated.

(Model I, Fig. 4 *A*) or the dissociation rate (Model II, Fig. 4 *B*). The original model (Huxley, 1957) has asymmetry in both: all three models produce a population of bound heads biased toward positive x and hence give net isometric tension in muscle. At low trap stiffness ($\kappa_t \ll$ k), Brownian motion is large and any strain-dependence of the "isometric" rates $f(x)$ and $g(x)$ is largely washed out, whereas when $\kappa_t \gg$ k these rate constants are preserved. Low values of f have been chosen to approximate the observed rates, which are lower than those expected in fibers; this may be due to unfavorable positions or orientations of the head with respect to F-actin. Nevertheless, the strain-dependences of $f(x)$ and $g(x)$ can be determined experimentally from level histograms at different resting dumbbell positions using Eqs. 16 and 17, and the results should discriminate between models I and II. Force rather than displacement data are preferable, because strain-dependent kinetics are preserved only at high trap stiffness where the Brownian motion of the filament is reduced.

Analogous predictions for the x-dependence of step sizes in A. F. Huxley's model can be understood by combining Eq. 19 with kinetic considerations, which select the most favorable binding site for each resting position. For $\kappa_t \ll$ k and a given value of x, Eq. 19 predicts quantized step sizes $-c-x$, $-x$, $\mathrm{c}-x$, ... proportional to x and separated by the monomer spacing $c = 5.5$ nm, but the frequency of these steps in the time record is controlled by the apparent binding constants $\tilde{K}(x + lc)$ for $l = -1,0,1,\ldots$. (Eq. 16), which show a single maximum. If the stiffness of the dumbbell with bound head is low, then these binding constants vary slowly with x and the binding range (defined, say, by $\tilde{K}(x) > 0.2\,\tilde{K}_{\max}$) may be larger than the site spacing. In that case, multiple steps arising from adjacent actin sites are statistically possible for each resting position (Fig. 5 *A*). If the cross-bridge is very stiff (k $>$ 2 pN/nm) and the traps also, then the binding range in x can be $<$5.5 nm so only one site is selected for each x (Fig. 5 *B*). The figure also shows that step sizes selected in this way are periodic in x modulo the site spacing; a 5.5 nm shift in resting position transfers the same cross-bridge kinetics to the next actin site. Hence the range of possible step sizes for *all* resting positions is kinetically selected and equal to the binding range.

DISCUSSION

Limitations of the model

An important limitation of the model is that internal Brownian motions of the myosin head and actin filament are not described explicitly, but absorbed in effective position-dependent rate constants of the cross-bridge cycle. This procedure is valid only if dumbbell motion is slower than significant internal motions. This can be demonstrated for any thermally activated reaction. Let the reaction rate be $k(x) = A \exp(-\Delta E(x)/\mathrm{RT})$ where A is the attempt frequency produced by internal motions and $\Delta E(x)$ the position-dependent energy barrier to binding (Kramers, 1940). The expo-

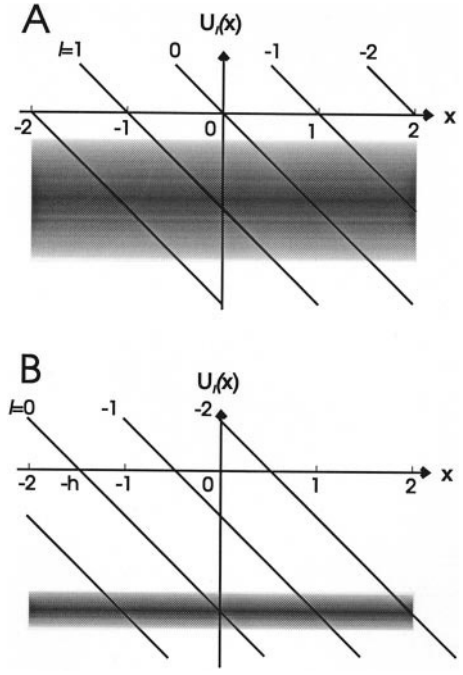

FIGURE 5 (*A*) The step size $U_l(x) = -k(x + h + lc)/(k + \kappa_t)$ in Huxley's model (Eq. 19) for binding to actin site l is determined by the resting position x of the dumbbell and varies linearly with x. The frequency of steps of each size is indicated by the degree of gray shading (shown for model I), proportional to the strength of myosin binding (Eq. 16). For the same x value, multiple step sizes separated by the actin site spacing c are possible if the binding range is large as shown. (*B*) With large cross-bridge stiffness and a force-generating transition after binding, the binding ranges in x are narrow and the step size is $-k(x + h + lc)/(k + \kappa_t)$, where h is the throw distance (Huxley and Simmons, 1971). In this case, step sizes are localized $\sim -kh/(k + \kappa_t)$ but realized only when the head is very close to an actin site. Distances are shown in units of $c = 5.5$ nm.

nential factor is the probability of the fluctuation giving virtually instantaneous bonding; this is the basis for the stochastic interpretation of chemical kinetics (Nicolis and Prigogine, 1977). In the presence of filament motion, x is a function of time so the probability of bonding at time t is $\exp(-\Delta E(x(t))/RT)$. The formula applies unchanged if the preceding motions in the potential well are undisturbed by moving the barrier, which must therefore vary slowly in comparison with the attempt frequency, that is, $d \ln \Delta E(x(t))/dt \ll A$. Thus a necessary condition for the validity of the Brownian dumbbell model is

$$\lambda(t) \ll A \tag{20}$$

where A is the frequency of the motion considered.

For myosin-S1, $A \sim 10^5\ s^{-1}$ if the head is detached (Thomas et al., 1980) and $10^7\ s^{-1}$ if the head is bound with ATP (Svensson and Thomas, 1986), which precedes dissociation from actin. The amplitudes of orientational fluctuations of the (tethered) detached head might be at least 20° (Svensson and Thomas, 1986). The actin filament with fixed ends undergoes thermally induced torsional and bending motions. Torsional relaxation frequencies in the range $10^{(4-5)}\ s^{-1}$ have been observed by Prochniewicz et al. (1996) and Yoshimura et al. (1984), while bending modes may be slower. Condition (20) is usually satisfied, as the corner frequency λ of displacement noise in current trap experiments is in the range $10^{(3-4)}\ s^{-1}$ (Table 1).

The elastic constants of the actin filament prohibit significant stretching and bending under the forces available (the cross-bridge or Brownian forces). The linear stiffness of a 1 μm regulated filament is 0.065N/m (Kojima et al., 1994) and the bending stiffness, which can be estimated from a torsional rigidity of 8×10^{-20} N · m (Tsuda et al., 1996), is similar. The r.m.s. lateral displacement of the middle of a fixed-end filament from thermally driven bending is estimated at $0.25\sqrt{L}$ nm (Doi and Edwards, 1988), where L is the length in microns. A similar estimate for thermally driven torsional oscillations gives an r.m.s. twist of $\sim 30\sqrt{L}°$, or 2° per protomer (a higher figure is found by Yoshimura et al.). These motions are likely to be important in determining the availability of binding sites to the head. However, under some conditions the whole actin-bead system might also rotate slowly about an axis through the trap centers, exposing more binding sites over the rotation period.

In Huxley's model Brownian motion of the detached head, its binding to actin, and subsequent isomerizations into a force-holding state are combined into a single process (Smith and Geeves, 1995). Force-holding states with different bound nucleotides are also combined. Thus, the composite binding rate $f(x)$ could be much less than the rate $k(x)$ for Brownian-induced binding to the initial attached state, but it is the latter whose pre-exponential factor sets an upper limit for the frequency of translational motion.

The unaveraged rate constants describing single-molecule experiments might differ from those in a muscle fiber with the same proteins and sarcoplasmic conditions. For example, unfavorable positioning of the dumbbell would lower the attempt frequency and give smaller binding rates $f(x)$ than exist in fibers. Tethering the myosin head to a coverslip might change its kinetics, either through electrostatic effects or by modifying the internal motions it can make. Torsional disorder in the thin filament may also be different in the two systems.

Is there a universal step size?

This simple Brownian dumbbell model predicts that step sizes, and bound-state lifetimes at high trap stiffness, vary with the resting position of the dumbbell. How are these predictions related to various claims for force pulses and displacement steps of fixed size, for example 5 pN/10 nm or greater (Finer et al., 1994; Ishijima et al., 1996) or 2 pN/5 nm (Molloy et al., 1995b)? The answer is probably a consequence of the kind of strain-dependent kinetics expected from fiber cross-bridge models, inadequate long-term position control, undesirable forms of mechanical compliance, and different methods of data analysis.

The binding range of myosin heads to a fixed actin filament is dependent on cross-bridge stiffness but is esti-

mated at ~10 nm for k = 0.5 pN/nm after phosphate is released (Smith and Geeves, 1995). This range can span two or possibly three neighboring actin sites, so multiple bound-state levels spaced by 5.5 nm are possible, particularly at low trap stiffness where the range is broadened by Brownian motion (Fig. 4). Displacement distributions of *selected* levels in displacement data of Molloy et al. (1995b) are spaced by ~11 nm and could therefore arise from next-nearest neighbor sites if additional levels at half that spacing are also present in the record. However, it is very difficult to achieve long-term stability of the trap positions to nanometer precision, so the predicted position dependences may be explored in an uncontrolled way, generating large steps only when the resting position favors the bound head. In these circumstances, displacement steps near the upper limit defined by the binding range (10 or 5 nm for k = 0.5, or 2 pN/nm, respectively), and corresponding force pulses (5 or 10 pN) should always be visible.

Cross-bridge model II of this paper predicts short-lived negative force pulses; if these arise from cycling cross-bridges they can always be prolonged by lowering the ATP concentration.

A fixed working stroke independent of the resting position of the dumbbell is possible if the cross-bridge is very stiff and there is a post-binding transition of the myosin head from a low-force to a high-force state (Huxley and Simmons, 1971). In this case, the binding stroke would be very small and the working stroke as defined earlier would be dominated by the second process. If nanometer position control could be achieved, this model would yield frequent steps only in small ranges of x values (Fig. 5 *B*), an extreme form of kinetic selection. However, the need for long-term position control could be avoided if it were known that the binding kinetics is selecting very narrow x-windows, as in Fig. 5 *B*. For example, all statistically identified steps of the same size in a long data run or pooled data should then correspond to a single value of x, or two or three discrete values spaced by 5.5 nm if the traps are weak. In the same way, pooled data for the lifetimes of the bound head may belong to a single x value provided their mean levels are the same to within sampling error, and this could be verified by testing for a Poisson distribution. The lifetimes of stepped regions with different levels should not be pooled, because if the level is kinetically selected then different levels would correspond to different x-values, whose mean lifetimes may be different (model II). The compliance of the actin filament (0.015 nm/pN per micron, Kojima et al., 1994) is insufficient to broaden the binding range in single-molecule experiments.

What determines the duty ratio?

The interpretation of force data is complicated by unwanted compliance in the actin-bead linkage, and a loss of trap stiffness at high frequencies when using a feedback system with finite bandwidth (R. M. Simmons, personal communication). Actin-bead compliance appears in series with cross-bridge compliance when the head is bound (Appendix A), and out-of-phase bead motions which distort these links are removed by averaging the position signals from each bead. Both forms of compliance could be responsible for some worrying features of single-molecule force data (Finer et al., 1994; Molloy et al., 1995b; Guilford et al., 1997). Duty ratios of under 0.01 for force pulses at physiological ATP levels are far lower than values near unity expected for the few positively strained heads in the sarcomere (themselves a small fraction of the total) which produce active tension in isometric muscle. The low duty ratio could be partly due to lower binding rates in single-molecule experiments, but mainly to rates of dissociation above 100 s^{-1} which are characteristic of negatively strained heads produced in shortening muscle, rather than rates of order 1 s^{-1} (phase 4) for tension-generating heads in isometric muscle (Smith, 1998). Similarly, trap data for the lifetime of the bound state (Molloy, 1995a) show only a modest increase with x, insufficient to give duty ratios near unity. Perhaps compliant bead linkages reduce the degree of strain-blocking of ADP release at positive strains. Alternatively, loss of trap stiffness at high frequencies may allow occasional large negative displacements which promote rapid dissociation from actin.

Computational methods for obtaining levels and dwell times from the time records are not the subject of this paper, but in fact the generalized Smoluchowski equations allow the construction of maximum-likelihood algorithms which do away with the need to identify levels and lifetimes. They will be presented elsewhere.

APPENDIX A

The effect of compliant actin-bead links

If the beads are loosely linked to the actin filament with stiffness $\kappa_L/2$ per link, then the displacements $u_1(t)$, $u_2(t)$, $u(t)$ of the beads and the filament from their resting positions in the absence of myosin are given by coupled Langevin equations

$$-\frac{\beta}{2}\frac{du_1}{dt} - \frac{\kappa_t}{2}u_1 + F_1(t) + \frac{\kappa_L}{2}(u - u_1) = 0$$

$$-\frac{\beta}{2}\frac{du_2}{dt} - \frac{\kappa_t}{2}u_2 + F_2(t) + \frac{\kappa_L}{2}(u - u_2) = 0$$

$$-\frac{\beta_A}{2}\frac{du}{dt} - \frac{\kappa_L}{2}(u - u_1) - \frac{\kappa_L}{2}(u - u_2) + F_A(t) - T(x + u, t) = 0, \quad \text{(A1)}$$

where β_A is the drag coefficient and F_A the Brownian force on the actin filament. The drag coefficient can be estimated by treating the filament as an ellipsoid of revolution (Happel and Brenner, 1983), and is rather small ($\beta_A/\beta \approx 0.06$ for a filament 1 μm long). Hence, the viscous relaxation time β_A/κ_L for longitudinal motions of actin with respect to the bead is likely to be 10^{-6} s or below. On any longer time scale the actin filament must be in

mechanical equilibrium at all times, so

$$u = \frac{u_1 + u_2}{2} + \frac{F_A(t) - T(x + u, t)}{\kappa_L} \tag{A2}$$

replaces the last equation of A1. Let $\tilde{u}(u_1 + u_2)/2$ and $w = u_2 - u_1$, which are the coordinates for in-phase and out-of-phase motions of the two beads. The remaining equations of motion yield uncoupled equations for the symmetric and antisymmetric modes of motion, namely

$$-\beta \frac{d\tilde{u}}{dt} - \kappa_t \tilde{u} + F(t) - T(x + u, t) = 0, \tag{A3a}$$

$$-\frac{\beta}{2} \frac{dw}{dt} - \frac{\kappa_l + \kappa_t}{2} w + F_2(t) - F_1(t) = 0 \tag{A3b}$$

where $F(t) = F_1(t) + F_2(t) + F_A(t)$ is the net Brownian force. Note that the modes are uncoupled only if both bead-filament links have the same stiffness, and that Eq. A3a is apparently of the same form as the original Langevin Eq. 1. However, the cross-bridge tension is a function of filament displacement u and not the average displacement $\tilde{u}$ of the beads. On using Eq. 2 and substituting $u = \tilde{u} + (F_A - T)/\kappa_L$, this Langevin equation can be rewritten as

$$-\beta \frac{d\tilde{u}}{dt} - \kappa_t \tilde{u} + \tilde{F}(t) - \tilde{T}(x + \tilde{u}, t) = 0 \tag{A4}$$

where $\tilde{T}(x, t)$ is given by Eq. 2 with k replaced by the stiffness

$$\tilde{k} = \frac{k\kappa_L}{k + \kappa_L} \tag{A5}$$

of the cross-bridge and bead linkages in series, and

$$\tilde{F}(t) = F_1(t) + F_2(t) + \left(1 - \frac{\tilde{k}}{\kappa_L} n(t)\right) F_A(t). \tag{A6}$$

where $n(t) = 1$ if myosin is bound and 0 otherwise. Equation A4 is equivalent to the original Langevin equation with an effective cross-bridge stiffness $\tilde{k}$. The Brownian force includes a small contribution from the filament which is reduced when myosin binds.

APPENDIX B

Steady-state solutions of generalized Smoluchowski equations

Numerical solutions can be obtained by a shooting method, since the steady-state form of Eqs. 8 defines a two-point boundary problem. The boundary conditions are that $P_j(u)$ and their first derivatives go to zero as $u \to \infty$, the second condition giving no net velocity at large displacements. The method is illustrated by writing the equations in vector form as

$$\frac{\partial \mathbf{P}(u, t)}{\partial t} = -\frac{\partial \mathbf{J}(u, t)}{\partial u} - \mathbf{M}(x + u)\mathbf{P}(u, t) = 0 \tag{B1}$$

where

$$\mathbf{J}(u, t) = -\beta^{-1} \frac{\partial \mathbf{V}(u)}{\partial u} P - D \frac{\partial P}{\partial u}$$

$$\equiv -D \exp\left(-\frac{\mathbf{V}(u)}{RT}\right) \frac{\partial}{\partial u}\left(\exp\left(\frac{\mathbf{V}(u)}{RT}\right)\mathbf{P}\right)$$

is the flux of dumbbells in an ensemble, using Einstein's relation $D = RT/\beta$. $\mathbf{M}(x)$ is a matrix of the rate constants $f(x)$ and $g(x)$, and $\mathbf{V}$ a diagonal matrix of the elastic potentials of Eq. 9. The solutions vary rapidly at large displacements because the Boltzmann factors tend to be preserved under nonequilibrium conditions. It is useful to define new variables

$$\mathbf{Q}(u) = \exp(\mathbf{V}(u)/RT)\mathbf{P}(u),$$

$$\mathbf{R}(u) = \exp(-\mathbf{V}(u)/RT) \frac{d\mathbf{Q}(u)}{du} \tag{B2}$$

which satisfy the coupled first-order differential equations

$$\frac{d\mathbf{Q}}{du} = \exp(\mathbf{V}(u)/RT)\mathbf{R}(u),$$

$$\frac{d\mathbf{R}}{du} = D^{-1}\mathbf{M}(x + u)\exp(-\mathbf{V}(u)/RT)\mathbf{Q}(u). \tag{B3}$$

The first boundary condition is satisfied if $\mathbf{Q}$ is finite at large u, while Eqs. B1–B3 can be used to rewrite the no-flux condition at infinity in the form

$$\int_{-\infty}^{\infty} \mathbf{M}(x + u)\mathbf{P}(u) = D[\mathbf{R}(\infty) - \mathbf{R}(-\infty)] = 0 \tag{B4}$$

which is satisfied if $\mathbf{R}(u) \to 0$ as $u \to \infty$. For vectors of dimension N (in the present problem $N = 2(1 + L)$) there are $2N$ asymptotic conditions on $\mathbf{R}$, which are sufficient to define a unique steady-state solution of the $2N$ first-order differential equations in B3.

Hence numerical integration can start from $\mathbf{R} = 0$ at some large negative value of u, varying the starting vector $\mathbf{Q}$ until $\mathbf{R} \to 0$ at large positive u. The solution can then be normalized as in Eq. 10. This method was implemented in Fortran 77 using the root-finding subroutine "newt" of Press et al. (1992) and a simple stiff differential-equation integrator using the Backward Euler method with Gauss-Jordan matrix inversion. The dominant influence of the Boltzmann factors $\exp(-\mathbf{V}(u)/RT)$ at large u guarantees that the method converges quickly and is very robust. For the parameters used in Fig. 3, the numerical solutions agree to graphical accuracy with the approximate forms from Eqs. 14, 16, and 17, significant deviations occurring only when f and/or g are raised by a factor of 100 or more.

I am grateful to Prof. R. M. Simmons for discussions and a careful reading of the manuscript, to Prof. R. Streater for useful comments on the steady-state solution of the Smoluchowski-Huxley equations, and for discussions with Drs. J. Molloy, P. Guilford, and A. Trombetta.

This work was supported by a grant from the Wellcome Trust.

REFERENCES

Block, S. M., and K. Svoboda. 1995. Analysis of high-resolution recordings of motor movement. *Biophys. J.* 68:230S–241S.

Brokaw, C. J. 1976. Computer simulation of movement generating cross-bridges. *Biophys. J.* 16:1013–1027.

Chandrasekhar, S. 1943. Stochastic problems in physics and astronomy. *Rev. Mod. Phys.* 15: 1–89.

Colquhoun, D., and A. G. Hawkes. 1977. Relaxation and fluctuations of membrane currents that flow through drug-operated ion channels. *Proc. R. Soc. Lond.* B199:231–262.

Cooke, R. 1987. The mechanism of muscle contraction. *Crit. Rev. Biochem.* 21:53–118.

Cooke, R. 1997. Actomyosin interaction in striated muscle. *Physiol. Rev.* 77:671–697.

Derenyi, I., and T. Vicsek. 1996. The kinesin walk: a dynamic model with elastically coupled heads. *Proc. Natl. Acad. Sci. USA.* 93:6775–6779.

Doi, M., and S. F. Edwards. 1988. The Theory of Polymer Dynamics. Oxford Science Publishers, .

Finer, J. T. R. M. Simmons, and J. A. Spudich. 1994. Single myosin molecule mechanics: piconewton forces and nanometer steps. *Nature.* 368:113–119.

Ford, L. E., A. F. Huxley, and R. M. Simmons. 1977. Tension responses to sudden length change in stimulated frog muscle fibres near slack length. *J. Physiol.* (*Lond.*). 269:441–515.

Gardner, C. 1985. A Handbook of Stochastic Methods for Physics, Chemistry and the Natural Sciences. Springer-Verlag, Berlin.

Gilbert, S. P., M. R. Webb, M. Brune, and K. A. Johnson. 1995. Pathway of processive ATP hydrolysis by kinesin. *Nature.* 373:671–676.

Gordon, A. M., A. F. Huxley, and F. J. Julian. 1966. The variation in isometric tension with sarcomere length in vertebrate muscle fibres. *J. Physiol. (Lond.).* 184:170–192.

Guilford, W. H., D. E. Dupuis, G. Kennedy, J. Wu, J. B. Patlak, and D. M. Warshaw. 1997. Smooth and skeletal muscle myosins produce similar unitary forces and displacements in the laser trap. *Biophys. J.* 72: 1006–1021.

Happel, J., and H. Brenner. 1983. Low Reynolds Number Hydrodynamics. Martinus-Nijhoff, The Hague.

Hibberd, M. C., and D. R. Trentham. 1986. Relationships between chemical and mechanical events during muscle contraction. *Annu. Rev. Biophys. Chem.* 15:119–161.

Holmes, K. C. 1997. The swinging lever-arm hypothesis of muscle contraction. *Curr. Biol.* 7:R112–R117.

Huxley, A. F. 1957. Muscle structure and theories of contraction. *Prog. Biophys. Biophys. Chem.* 7:255–318.

Huxley, A. F., and R. M. Simmons. 1971. Proposed mechanism of force generation in striated muscle. *Nature.* 233:533–538.

Ishijima, A., T. Doi, K. Sakurada, and T. Yanagida. 1991. Sub-piconewton force fluctuations of actomyosin in vitro. *Nature.* 352:301–306.

Ishijima, A., H. Kojima, H. Higuchi, Y. Harada, T. Funatsu, and T. Yanagida. 1996. Multiple- and single-molecule analysis of the actomyosin motor by nanometer-piconewton manipulation with a microneedle: unitary steps and forces. *Biophys J.* 70:383–400.

Kojima, H., A. Ishijima, and T. Yanagida. 1994. Direct measurement of stiffness of single actin filaments with and without tropomyosin by in vitro manipulation. *Proc. Natl. Acad. Sci. USA.* 91:12962–12966.

Kramers, H. 1940. Brownian motion in a field of force and the diffusion model of chemical reactions. *Physica.* 7:284–304.

Ma, Y. Z., and E. W. Taylor. 1997. Interacting head mechanism of microtubule-kinesin ATPase. *J. Biol. Chem.* 272:724–730.

Molloy, J. E., J. E. Burns, J. Kendrick-Jones, R. T. Tregear, and D. C. S. White. 1995b. Movement, and force produced by a single myosin head. *Nature.* 378:209–212.

Molloy, J. E., J. E. Burns, J. C. Sparrow, R. T. Tregear, J. Kendrick-Jones, and D. C. S. White. 1995a. Single molecule mechanics of heavy meromyosin and S1 interacting with rabbit or Drosophila actins using optical tweezers. *Biophys. J.* 68:298S–305S.

Molloy, J. E., and D. C. S. White. 1997. Smooth and skeletal muscle single-myosin mechanical experiments. *Biophys. J.* 72:984–986.

Nicolis, G., and I. Prigogine. 1977. Self-Organization in Nonequilibrium Systems. J. Wiley and Sons, New York.

Pate, E., and R. Cooke. 1991. Simulation of stochastic processes in motile crossbridge systems. *J. Muscle Res. Cell Motil.* 12:376–393.

Peskin, C. S., and G. Oster. 1995. Coordinated hydrolysis explains the mechanical behavior of kinesin. *Biophys. J.* 68:202s–211s.

Press, W. H., S. A. Teukolsky, W. T. Vetterling, and B. R. Flannery. 1992. Numerical Recipes in Fortran. 2nd ed. Cambridge, United Kingdom.

Prochniewicz, E., Q. N. Zhang, E. C. Howard, and D. D. Thomas. 1996. Microsecond rotational dynamics of actin-spectroscopic detection and theoretical simulation. *J. Mol. Biol.* 255:446–457.

Reif, F. 1965. Fundamentals of Statistical and Thermal Physics. McGraw Hill, New York.

Saldana, R. P., and D. A. Smith. 1991. Four aspects of creep phenomena in striated muscle. *J. Muscle Res. Cell Motil.* 12:517–531.

Simmons, R. M., Finer, J. T., Chu, S., and Spudich, J. A. 1996. Quantitative measurements of force and displacement in the optical trap. *Biophys. J.* 70, 1813–1822.

Simmons, R. M., J. T. Finer, H. M. Warrick, B. Kralik, S. Chu, and J. A. Spudich. 1993. Force on single actin filaments in a motility assay measured with an optical trap. *In* Mechanism of Myofilament Sliding in Muscle Contraction, H. Sugi and G. H. Pollack, editors. Plenum Press, New York.

Smith, D. A. 1998. A strain-dependent ratchet model for [phosphate]- and [ATP]-dependent muscle contraction. *J. Muscle Res. Cell Motil.* 19: 189–211.

Smith, D. A., and M. A. Geeves. 1995. Strain-dependent crossbridge cycle for muscle. *Biophys. J.* 69:524–537.

Svensson, E. C., and D. D. Thomas. 1986. ATP induces microsecond rotational motions of myosin heads crosslinked to actin. *Biophys. J.* 50:999–1002.

Svoboda, K., and S. M. Block. 1994. Biological applications of optical forces. *Ann. Rev. Biophys. Biomol. Struct.* 23:247–285.

Svoboda, K., P. Mitra, and S. Block. 1994. Fluctuation analysis of motor protein movement and single enzyme kinetics. *Proc. Natl. Acad. Sci. USA.* 91:11782–11786.

Svoboda, K., C. F. Schmidt, B. J. Schnapp, and S. M. Block. 1993. Direct observation of kinesin stepping by optical trapping interferometry. *Nature.* 365:721–727.

Thomas, D. D., S. Ishiwata, J. C. Seidel, and J. Gergely. 1980. Submillisecond rotational dynamics or spin-labeled myosin heads in myofibrils. *Biophys. J.* 32:873–890.

Thomas, N., and R. A. Thornhill. 1995. A theory of tension fluctuations due to muscle cross-bridges. *Proc. R. Soc. (Lond.). B.* 259:235–242.

Tsuda, Y., H. Yasutake, A. Ishijima, and T. Yanagida. 1996. Torsional rigidity of single actin filaments and actin-actin bond breaking force under torsion measured directly by in vitro manipulation. *Proc. Natl. Acad. Sci. USA.* 93:12937–12942.

Weatherburn, C. E. 1968. A First Course in Mathematical Statistics. Cambridge, United Kingdom.

Yoshimura, H., T. Nishio, and K. Mihashi. 1984. Torsional motion of eosin-labeled F-actin as detected in the time-resolved anisotropy decay of the probe in the submillisecond time range. *J. Mol. Biol.* 179: 453–467.